RESEARCH

Genetic Analysis of Visually Scored Orange Kernel Color in Maize

Kristin Chandler, Alexander E. Lipka, Brenda F. Owens, Huihui Li, Edward S. Buckler, Torbert Rocheford,* and Michael A. Gore*

ABSTRACT

Increasing levels of provitamin A carotenoids in maize (*Zea mays* L.) grain through plant breeding has potential to help humans suffering from vitamin A deficiency. In parts of Africa where this deficiency is prevalent, there is a consumer preference for white maize grain and an avoidance of yellow maize grain. White grain has minimal levels of carotenoids whereas yellow grain can have appreciable levels of carotenoids. There is a new effort to introduce orange maize that contains high levels of provitamin A, which appears to be a more acceptable color than yellow to consumers in Africa. The implementation of this program requires backcross selection to convert African-adapted germplasm with white grain to orange. We conducted a study to assess the heritability of visual scores for relative intensity of orange kernel color and identify genetic markers associated with orange color across and within 10 families of the maize nested association mapping population. We found visually scored kernel color to have a moderately high heritability and identified five common quantitative trait loci (QTL) and six rare QTL for intensity of orange color. Notably, half of them coincided with carotenoid biosynthetic genes. Our results indicate that breeders in Africa, Asia, and throughout the world would have flexibility to select for orange kernel color visually and/or with gene-specific markers. Such selection can be combined with marker-assisted selection efforts to increase provitamin A levels in maize grain.

K. Chandler, B. Owens, and T. Rocheford, Department of Agronomy, Purdue University, West Lafayette, IN; A.E. Lipka, USDA-ARS, Robert W. Holley Center for Agriculture and Health, Ithaca, NY; H. Li, Institute of Crop Science, The National Key Facility for Crop Gene Resources and Genetic Improvement, Chinese Academy of Agricultural Sciences, Beijing, China; E.S. Buckler, USDA-ARS, Robert W. Holley Center for Agriculture and Health, Institute for Genomic Diversity, Department of Plant Breeding and Genetics, Cornell University, Ithaca, NY; M.A. Gore, USDA-ARS, U.S. Arid Land Agricultural Research Center, Maricopa, AZ; Current Address: K. Chandler, Pioneer, Hi-Bred International, Inc., 4200 West Service Road, Unit 4, Evans, CO 80620. K. Chandler and A.E. Lipka contributed equally to this work. *Corresponding authors (Torbert@purdue.edu; Michael.Gore@ars.usda.gov).

Abbreviations: AR1, first-order autoregressive; BLUP, best linear unbiased predictor; CCD, carotenoid cleavage dioxygenase; FDR, false discovery rate; $\hat{h}^2_c$, heritability across the entire experiment; $\hat{h}^2_l$, heritability on a line-mean basis across all nested association mapping families; $\hat{h}^2_{lw_p}$, heritability on a line-mean basis within only the *p*th nested association mapping family; $\hat{h}^2_p$, heritability on an individual plot basis across all nested association mapping families; MAS, marker-assisted selection; NAM, nested association mapping; PVE, phenotypic variance explained; Q×E, quantitative trait loci × environment; QTL, quantitative trait loci/locus; RIL, recombinant inbred line; SNP, single nucleotide polymorphism; ZEP, zeaxanthin epoxidase.

For millions of people in developing countries, plant products with dietary provitamin A carotenoids such as β-carotene, β-cryptoxanthin, and α-carotene are the major source of vitamin A (West and Darnton-Hill, 2008). Within these countries, insufficient provitamin A or vitamin A content in diets is a major cause

Published in Crop Sci. 53:189–200 (2013).
doi: 10.2135/cropsci2012.02.0129

of vitamin A deficiency. Complications associated with a deficiency in vitamin A include blindness, impaired growth and development, lowered immunity, and ultimately death (Underwood and Arthur, 1996). More than 7.2 million pregnant women and approximately 127 million preschool-aged children are vitamin A deficient in developing countries (West, 2002). Of the 5 to 10 million children that develop xerophthalmia (or dry eyes) from vitamin A deficiency, an estimated 250,000 to 500,000 of them become blind every year (Sommer, 1995; Sommer et al., 1981). Vitamin A deficiency is the central cause of more than 600,000 early childhood deaths each year (West and Darnton-Hill, 2008).

Vitamin A deficiency can be prevented by including sources of provitamin A or vitamin A in the diet. Supplementation, food fortification, and diet diversification have been used to try and address vitamin A deficiency (Mora, 2003; Ross, 2002; West, 2000; West et al., 2002). However, poverty, inadequate infrastructure, and other complicating factors within developing countries have limited the success of these approaches (Graham et al., 2001). Increasing the concentration of provitamin A in the edible portions of staple crops through plant breeding, termed biofortification, may have greater promise to reduce the incidence of vitamin A deficiency. This approach has the potential to be highly sustainable and cost effective when biofortified crops are continuously consumed and grown year after year at recurrent costs lower than the initial costs of varietal development (Bouis and Welch, 2010; Welch and Graham, 2004).

Maize is an important staple crop in many of the sub-Saharan African and Latin American countries where vitamin A deficiency is prevalent. Carotenoids in maize kernels produce colors ranging from light yellow to dark orange, and they are concentrated primarily in the vitreous (horny) portion of the endosperm (Weber, 1987). Darker orange kernels in maize tend to have higher total carotenoid concentrations compared to lighter orange and yellow kernels (Harjes et al., 2008), but most of the higher total concentration results from non-provitamin A xanthophyll carotenoids (Quackenbush et al., 1961; Weber, 1987). Even though considerable variation exists for total carotenoids levels in maize kernels, Harjes et al. (2008) showed that the majority of yellow kernel maize inbred lines from a global collection do not have enough provitamin A (average of 1.7 $\mu g\ g^{-1}$ β-carotene) to meet recommended dietary allowance levels for adequate nutrition (Institute of Medicine, 2012).

White maize is highly preferred over yellow maize for human consumption in East and southern Africa (De Groote and Kimenju, 2008; Pillay et al., 2011). The perceived inferiority of yellow maize is due in part to its negative association with imported relief food and unfavorable taste and texture (Muzhingi et al., 2008). However, recent studies are showing that there does not appear to be strong aversion to orange maize. In Mozambique, orange maize was shown to be an acceptable product to consumers and its aroma was even preferred to that of a local white maize variety (Stevens and Winter-Nelson, 2008). In rural Zambia, the provision of nutrition information resulted in consumers putting a slightly higher premium on orange maize than on white maize (Meenakshi et al., 2012). Taken together, these studies show that with appropriate consumer education efforts the introduction of orange maize for reducing vitamin A deficiency would likely be successful in Africa.

As orange maize grain becomes accepted by African consumers, maize breeding programs in Africa will need to rapidly convert locally adapted, high-yielding white grain open-pollinated varieties and hybrids without endosperm carotenoids to orange color with substantial levels of total carotenoids. Orange kernel color tends to have a moderate positive correlation with total carotenoids but only a very weak positive correlation with provitamin A carotenoids (Harjes et al., 2008). Therefore, continual selection for darker orange color, which should result in higher levels of total carotenoids, will need to be accompanied by marker-assisted selection (MAS) to specifically increase the proportion of provitamin A carotenoids. Presently, MAS for favorable alleles of the carotenoid biosynthetic genes *lcyE* (lycopene epsilon cyclase) (Harjes et al., 2008) and *crtRB1* (β-carotene hydroxylase 1) (Yan et al., 2010) has been shown to increase levels of provitamin A (Kandianis, 2009) and is now being used together with high-performance liquid chromatography analysis by HarvestPlus maize breeders to more efficiently develop inbred and hybrids with higher provitamin A levels (K. Pixley, HarvestPlus and CIMMYT, personal communication, 2012).

Maize breeding programs in Africa, Asia, and throughout the world where it would be beneficial to increase the nutritional content of grain will benefit from rapid, convenient methods to convert locally adapted, superior performing white or yellow grain germplasm to orange color with high total carotenoids. We conducted the present study to (i) evaluate the extent to which visual scores for gradation in orange kernel color are heritable and (ii) identify quantitative trait loci (QTL) associated with orange color phenotypes in 10 families from the maize nested association mapping (NAM) population.

MATERIALS AND METHODS

Germplasm

The germplasm selection process, design, and construction of the maize NAM population have been previously described (Buckler et al., 2009; McMullen et al., 2009; Yu et al., 2008). The maize NAM population consists of 25 families of 200 recombinant inbred lines (RILs) per family resulting in a total of 5000 RILs. Maize inbred line B73 was crossed in a reference design

Figure 1. Standardized color scale that included representative kernels from all 10 nested association mapping families in 2009 and 2010. The ordinal color scale ranges from 1 (lightest yellow) to 12 (darkest orange).

to 25 other diverse inbred lines and 200 RILs were developed from each cross. We identified and studied 10 NAM families that segregated for gradation in orange kernel color: B73 × B97, B73 × CML228, B73 × CML52, B73 × Hp301, B73 × Ki11, B73 × Ki3, B73 × NC350, B73 × NC358, B73 × Oh7B, and B73 × Tx303. Populations segregating for sweetness (*su1*) were excluded from the analysis (B73 × Il14H and B73 × P39) because the wrinkly texture of *su1* kernels made it very difficult to score their kernel color with the identical standardized color scale that was used for other non-sweet corn populations.

Construction of a linkage map with 1106 single nucleotide polymorphism (SNP) markers for the maize NAM population has been previously described (McMullen et al., 2009). Briefly, RILs were genotyped with a panel of 1536 SNPs by the Illumina GoldenGate Assay system (Illumina, Inc.). The panel consisted of SNPs that were selected from randomly chosen genes (~64%), candidate genes that potentially control phenotypic variation for agronomic traits (~21%), and sequence alignments provided by Pioneer Hi-Bred International (~15%). Missing SNP marker genotypes at the 1106 marker loci were imputed as previously described in Tian et al. (2011) because joint and single family linkage analyses with stepwise regression cannot use RILs that have missing marker data.

Phenotypic Evaluation

The 5000 NAM RILs, 200 randomly selected intermated B73 × Mo17 RILs (Lee et al., 2002), and an association mapping panel of 281 diverse inbred lines (Flint-Garcia et al., 2005) were grown in the summers of 2009 and 2010 at the Agronomy Center for Research and Education in West Lafayette, IN. The experimental field design has been previously described (Hung et al., 2012). Briefly, the experimental layout in each environment was a sets design, wherein each set included all lines of a family or the association population. Each family set was arranged as a 10 × 20 incomplete block α-lattice design. The α-design was augmented by including both parental lines of a family as checks within each incomplete block. The association mapping population was arranged as a 14 × 20 incomplete block α-lattice design, and each incomplete block was augmented by the addition of B73 and Mo17. Within each of the two environments, a single replicate of the entire experiment of 5481 unique lines plus parental checks was grown in one-row plots. Experimental units consisted of a single line in a 3.05-m one-row plot, and each plot had an average of 10 plants. In 2009, all plants within a plot were self-pollinated by hand because of the need to increase seed for planting in 2010 and subsequent years. Only four plants per plot were self-pollinated by hand in 2010. Pollinated ears were harvested at maturity and dried to about 15% moisture content. Subsequently, the harvested ears of each plot were shelled and bulked to form a representative, composite sample for phenotyping.

Joint linkage analysis requires the phenotyping of all families on an identical scale. Therefore, each bulk of kernels was visually scored for kernel color by comparing to a standardized color scale that included representative kernels from all 10 NAM families in 2009 and 2010. The ordinal color scale had a range of 12 categorical colors (Fig. 1), with 1 the lightest yellow and 12 the darkest orange. Kernels were scored with the embryo face down. The bulk from each plot consisted of at least 100 kernels, but the total number of kernels per bulk varied. Therefore, kernels within a bulk were grouped by color and each color group was assigned a score. Most bulks were uniform in color, but some segregated for multiple kernel colors. Segregating bulks were scored as an average of observed kernel colors. Each bulk from NAM families was scored once by one person (Kristin Chandler). Bulked samples that had discolored kernels due to fungal infection or other opportunistic pathogens were not scored. If kernel color was difficult to unambiguously score or the pericarp was colored with anthocyanin pigments, the pericarp of kernels was removed.

Phenotypic Data Analysis

Best linear unbiased predictors (BLUPs) of kernel color for each line were predicted from a random effects model analysis across environments per Hung et al. (2012) in ASReml version 3.0 (Gilmour et al., 2009):

$$\begin{aligned} Y_{ijklmnop} = {} & \mu + \text{env}_i + \text{field(env)}_{ij} + \text{set(field} \times \text{env)}_{ijk} \\ & + \text{block(set} \times \text{field} \times \text{env)}_{ijkl} \\ & + \text{row(field} \times \text{env)}_{ijm} + \text{column(field} \times \text{env)}_{ijn} \\ & + \text{family}_o + (\text{env} \times \text{family})_{io} + \text{RIL(family)}_{op} \\ & + [\text{env} \times \text{RIL(family)}]_{iop} + \varepsilon_{ijklmnop}, \end{aligned} \quad [1]$$

in which $Y_{ijklmnop}$ is an individual observation, μ is the overall mean, env_i is the effect of the *i*th environment, field(env)_{ij} is the effect of the *j*th field within the *i*th environment (two fields were used in 2009), $\text{set(field} \times \text{env)}_{ijk}$ is the effect of the *k*th set within the *j*th field within the *i*th environment, $\text{block(set} \times \text{field} \times \text{env)}_{ijkl}$ is the effect of the *l*th incomplete block within the *k*th set within the *j*th field within the *i*th environment, $\text{row(field} \times \text{env)}_{ijm}$ is the effect of the *m*th plot grid row direction within the *j*th field within the *i*th environment, $\text{column(field} \times \text{env)}_{ijn}$ is the effect of the *n*th plot grid column within the *j*th field within the *i*th environment, family_o is the effect of the *o*th family, $\text{env} \times \text{family}_{io}$ is the effect of the interaction between the *o*th family and the *i*th environment, RIL(family)_{op} is the effect of the *p*th RIL within the *o*th family, $\text{env} \times \text{RIL(family)}_{iop}$ is the effect of the interaction between the *p*th RIL within the *o*th family and the *i*th environment, and $\varepsilon_{ijklmnop}$ is the random error term. A first-order autoregressive (AR1 ×

AR1) correlation structure was used to account for spatial variation among the rows and columns.

Likelihood ratio tests were conducted to remove all terms from the model that were not significant at $\alpha = 0.05$ (Littell et al., 1996). The row and column main effects as well as the first-order autoregressive (AR1 × AR1) correlation structure were not statistically significant. Therefore, they were not included in the final model. The final model was used to estimate BLUPs for each line and to estimate variance components (Supplemental Table S1). Subsequently, these variance components were used to estimate heritabilities. Unique error variances were modeled for each environment. In addition, unique genetic and genetic × environment variance components were fitted for each NAM family.

Heritability Estimation

Heritability on an individual plot basis across all NAM families ($\hat{h}_p^2$) (Holland et al., 2003; Hung et al., 2012) was estimated across the 10 NAM families as follows:

$$\hat{h}_p^2 = \left[\hat{\sigma}^2_{\text{family}} + (1/10)\sum_{p=1}^{10}\hat{\sigma}^2_{\text{RIL(family)}_p}\right] \Bigg/ \left\{\begin{array}{l}\hat{\sigma}^2_{\text{family}} + \left[(1/10)\sum_{p=1}^{10}\hat{\sigma}^2_{\text{RIL(family)}_p}\right] \\ \quad + \left[(1/2)\sum_{q=1}^{2}\hat{\sigma}^2_{\text{env}_q\times\text{family}}\right] \\ \quad + \left[(1/20)\sum_{p=1}^{10}\sum_{q=1}^{2}\hat{\sigma}^2_{\text{env}_q\times\text{RIL(family)}_p}\right] + \hat{\sigma}^2_{\varepsilon}\end{array}\right\}, \quad [2]$$

in which $\hat{\sigma}^2_{\text{family}}$ is the variance component estimate for family, $\hat{\sigma}^2_{\text{RIL(family)}_p}$ is the variance component estimate of the RILs within the pth family, $\hat{\sigma}^2_{\text{env}_q\times\text{family}}$ is the variance component estimate of the two-way interaction between the qth environment and family, $\hat{\sigma}^2_{\text{env}_q\times\text{RIL(family)}_p}$ is the variance component estimate for the two-way interaction between the qth environment and RILs within the pth family, and $\hat{\sigma}^2_e$ is the residual variance component estimate.

Heritability on a line-mean basis across all NAM families ($\hat{h}_l^2$) (Holland et al., 2003; Hung et al., 2012) was estimated as follows:

$$\hat{h}_l^2 = \left[\hat{\sigma}^2_{\text{family}} + (1/10)\sum_{p=1}^{10}\hat{\sigma}^2_{\text{RIL(family)}_p}\right] \Bigg/ \left\{\begin{array}{l}\hat{\sigma}^2_{\text{family}} + \left[(1/10)\sum_{p=1}^{10}\hat{\sigma}^2_{\text{RIL(family)}_p}\right] \\ \quad + \left\{\left[(1/2)\sum_{q=1}^{2}\hat{\sigma}^2_{\text{env}_q\times\text{family}}\right] / n_{\text{env}_f}\right\} \\ \quad + \left\{\left[(1/20)\sum_{p=1}^{10}\sum_{q=1}^{2}\hat{\sigma}^2_{\text{env}_q\times\text{RIL(family)}_p}\right] / n_{\text{env}_l}\right\} \\ \quad + \left(\hat{\sigma}^2_{\varepsilon} / n_{\text{plot}}\right)\end{array}\right\}, \quad [3]$$

in which n_{env_f} is the harmonic mean of the number of environments in which each family was observed, n_{env_l} is the harmonic mean of the number of environments in which each line was observed, n_{plot} is the harmonic mean of the number of plots in which each line was observed, and all remaining terms are as previously defined.

Heritability on a line-mean basis within only the pth NAM family ($\hat{h}^2_{lw_p}$) (Hung et al., 2012) was estimated as follows:

$$\hat{h}^2_{lw_p} = \hat{\sigma}^2_{\text{RIL(family)}_p} \Bigg/ \left\{\begin{array}{l}\hat{\sigma}^2_{\text{RIL(family)}_p} \\ \quad + \left\{\left[(1/2)\sum_{q=1}^{2}\hat{\sigma}^2_{\text{env}_q\times\text{RIL(family)}_p}\right] / n_{\text{env}_{lp}}\right\} \\ \quad + \left(\hat{\sigma}^2_{\varepsilon} / n_{\text{plot}_p}\right)\end{array}\right\}, \quad [4]$$

in which $n_{\text{env}_{lp}}$ is the harmonic mean of the number of environments in which each line was observed for each family, n_{plot_p} is the harmonic mean of the number of plots in which each line was observed for each family, and all remaining terms are as previously defined. The standard errors of heritability estimates Eq. [2], Eq. [3], and Eq. [4] were approximated with the delta method (Holland et al., 2003).

The heritability across the entire experiment ($\hat{h}^2_C$) (Cullis et al., 2006) was estimated as follows:

$$\hat{h}^2_C = 1 - V_{\text{PPE}} / \left[2\left(\hat{\sigma}^2_{\text{family}} + \hat{\sigma}^2_{\text{RIL}\times\text{(family)}}\right)\right], \quad [5]$$

in which V_{PPE} is the average prediction error variance among all pairwise comparisons.

Joint Linkage Analysis

The joint linkage analysis procedure of Buckler et al. (2009) combines information across all included families of the NAM population to identify and position QTL. Briefly, we identified QTL in a combined analysis of the 10 NAM families by implementing a joint stepwise regression procedure where the data set of kernel color trait BLUPs was the response variable, the family main effect was an explanatory variable, and 1106 SNP markers were considered for explanatory variables in the final model. A family main effect was fit first in the joint stepwise regression model followed by the selection of marker effects nested within families to enter or exit the model based on the P-value calculated for a partial F-test in SAS version 9.2 (SAS Institute, 2011). A permutation procedure (Churchill and Doerge, 1994) was run 1000 times to control the type I error rate at $\alpha = 0.05$. The resulting 1000 P-values were sorted, and the 50th smallest P-value, 8.74×10^{-7}, was selected as the empirical $\alpha = 0.05$ entry threshold. To prevent a marker from entering and exiting the model during the same step, the exit threshold was set to twice the value of the entry threshold, namely 1.76×10^{-6}. Joint linkage QTL support intervals were calculated as previously described (Tian et al., 2011). Within each QTL identified by stepwise regression, t tests were conducted to determine the significance of QTL effects for each family. The Benjamini–Hochberg (1995) procedure was used to control the false discovery rate (FDR) at 5% when identifying potentially significant QTL effects. The phenotypic variance explained (PVE) by each QTL in the NAM population was calculated as described in Li et al. (2011).

Single Family Linkage Analysis

The single family linkage analysis procedure of Buckler et al. (2009) uses only information within an individual family to identify and locate QTL. Briefly, we identified QTL in each of the single NAM families by fitting a linkage model using stepwise regression of kernel color trait BLUPs on 1106 SNP markers. Marker effects entered or exited the model based on the significance level chosen from running a permutation procedure 1000 times for each family (Churchill and Doerge, 1994). We calculated support intervals for each QTL per Tian et al. (2011). The PVE by each QTL within each NAM family was calculated as described in Li et al. (2011).

Epistasis

We tested for epistatic interactions among all possible pairs of 1106 SNP markers in a combined analysis across the 10 NAM families as previously described (Buckler et al., 2009). Briefly, for each pair of markers, a family main effect, the main effect of each marker in the pair nested within family, and the interaction term of the marker pair nested within family were fitted as fixed effects in the model. Selected marker pairs were combined with the NAM joint linkage additive QTL model and formally tested for significant epistatic interaction across families at $\alpha = 0.05$. To test for epistatic interactions within families separately, the statistical analysis was identical to that used for the joint analysis combined across families, with the exception that the two main marker effects and one marker interaction were not nested within families. Statistical significance was determined at $\alpha = 0.05$. The Benjamini–Hochberg (1995) procedure was used to control the FDR at 5% when identifying potentially significant interaction terms in the joint and single family analyses.

Quantitative Trait Loci × Environment Interactions

We evaluated QTL × environment (Q×E) interactions across the 10 NAM families using BLUPs for each line that were calculated separately for each environment. This Q×E analysis procedure is described in Buckler et al. (2009). Briefly, a general linear model was fitted that contained these BLUPs as the response variable; family, environment, family × environment, the main effects of all significant QTL, and the Q×E interaction for each significant QTL were included as the explanatory variables. Each Q×E term was tested, and the Bonferroni correction was used to control the familywise type I error rate at $\alpha = 0.05$. Subsequently, significant Q×E interaction terms were included in a reduced mixed model that refitted both QTL and Q×E effects as random terms in ASReml version 3.0 (Gilmour et al., 2009).

RESULTS

Phenotypic Variability

We investigated the extent to which gradation in orange kernel color score varied across 10 families from the maize NAM population. Kernels from approximately 2,000 RILs plus replicated parental checks were visually scored for kernel color for 2 yr at a single location (Fig. 1), and the collected phenotypic values were used to calculate BLUPs over the two environments. The common reference parent B73 had a lower kernel color BLUP than all of the diverse NAM founder parents except for B97 (Table 1). The four families with the highest mean kernel color BLUP were B73 × Ki11, B73 × CML52, B73 × Ki3, and B73 × Hp301. Significant transgressive variation ($\alpha = 0.05$) existed in both directions in the B73 × NC350 family, and significant positive transgressive variation ($\alpha = 0.05$) was present in the B73 × CML228 family (Table 1). None of the positive transgressive variants from these two families had a kernel color BLUP greater than Ki11, the diverse parent with darkest orange kernel color.

Heritability on a line-mean basis across all NAM families ($\hat{h}_l^2$) corresponds to the maximum level of phenotypic variability among lines from the 10 NAM families that can be attributed to the combined effects of QTL (Hung et al., 2012). Kernel color had a moderately high line-mean basis heritability ($\hat{h}_l^2 = 0.78$, SE = 0.05) across 2 yr at a single

Table 1. Means and ranges of kernel color best linear unbiased predictors (BLUPs) for 10 families of the maize nested association mapping (NAM) population, midparent values, transgressive variation, and estimated heritability on a line-mean basis within only the *p*th NAM family ($\hat{h}^2_{lw_p}$) with their SE in two summer environments, in West Lafayette, IN, across 2 yr.

	Families			Parent means			Transgressive variation		Heritabilities	
Pedigree	No. RILs†	Mean	Range	B73	Diverse parent	Midparent	Negative‡	Positive§	$\hat{h}^2_{lw_p}$	SE ($\hat{h}^2_{lw_p}$)
B73 × B97	192	5.51	4.29–6.15	5.60	4.69	5.14	–	–	0.44	0.09
B73 × CML228	181	7.35	5.17–10.47	5.60	8.12	6.86	–	9	0.77	0.04
B73 × CML52	140	7.63	5.18–9.89	5.60	10.86	8.23	–	–	0.68	0.05
B73 × Hp301	188	7.51	5.87–8.74	5.60	10.12	7.86	–	–	0.63	0.04
B73 × Ki11	187	8.12	5.57–10.25	5.60	11.95	8.77	–	–	0.71	0.04
B73 × Ki3	175	7.53	5.59–10.50	5.60	10.40	8.00	–	–	0.81	0.03
B73 × NC350	179	5.50	3.06–9.00	5.60	6.96	6.28	23	2	0.81	0.03
B73 × NC358	180	6.36	5.06–7.74	5.60	9.17	7.38	–	–	0.44	0.07
B73 × Oh7B	183	6.07	4.77–7.28	5.60	6.94	6.27	–	–	0.54	0.07
B73 × Tx303	194	5.68	3.94–7.17	5.60	7.45	6.52	–	–	0.53	0.06

†RIL, recombinant inbred line.

‡Number of RILs with a kernel color BLUP less than that of the lowest parent at $\alpha = 0.05$.

§Number of RILs with a kernel color BLUP greater than that of the highest parent at $\alpha = 0.05$.

location, indicating that sufficient statistical power and precision exists for QTL mapping and effect estimation. The estimated heritability of kernel color on an individual plot basis ($\hat{h}_p^2$ = 0.69, SE = 0.06), where plot (one-row) was an unreplicated experimental unit that consisted of a single line, was only slightly lower than $\hat{h}_l^2$. Estimated $\hat{h}_{lw_p}^2$ ranged from 0.44 for B73 × B97 to 0.81 for B73 × Ki3 and B73 × NC350, with the mean of all families at 0.64 (Table 1). Heritability for the combined 10 NAM families and repeated parental check lines ($\hat{h}_C^2$ = 0.87) was 23% higher than the average of individual within-family heritabilities, which represents genetic variation attributable to the diverse parents.

Quantitative Trait Loci Analysis

We mapped QTL for gradation in orange kernel color in a combined analysis of the 10 NAM families using a joint stepwise regression procedure. This procedure is statistically more powerful when QTL segregate in multiple families (i.e., common QTL) (Li et al., 2011). The joint linkage analysis identified five QTL that accounted for approximately 76% of the total variance for kernel color and approximately 97% of genetic variance (Table 2). The PVE by individual QTL across NAM families ranged from approximately 5 to 38%. A QTL on chromosome 8 explained the largest proportion of phenotypic variance for kernel color followed by QTL on chromosomes 6, 9, and 2.

Joint linkage analysis allowed us to estimate a separate effect at each of the five QTL for all 10 families. Only 23 out of a possible 50 identified QTL across the 10 families had significant effects (FDR = 5%) relative to B73 (Fig. 2). Of the 23 QTL with a significant effect, 19 QTL had a positive effect for increased orange color relative to B73 while the other four QTL had a negative effect for decreased orange color. Quantitative trait loci on chromosomes 8 and 9 (98.2 cM) had both positive and negative effects across the 10 NAM families (Fig. 2). Only three of the 23 QTL had an estimated effect larger than 5% while the other 20 QTL were estimated to give an increase or decrease of approximately plus or minus 1 to 5% color score units (Fig. 3).

We conducted QTL analysis within each of the 10 families using stepwise regression. In general, single family linkage analysis has less precision and statistical power than joint linkage analysis for identifying common QTL (Li et al., 2011). However, there are instances when single family linkage analysis offers higher power to detect rare QTL segregating in a single family. The number of significant QTL identified for each family ranged from one to five (Table 3). We identified two rare QTL for B73 × Tx303 and one rare QTL each for B73 × B97, B73 × Ki3, B73 × NC350, and B73 × Oh7B that were not identified with joint linkage analysis. Additional QTL, but with a test statistic that was below the significance threshold level, were detected in most families in the same genomic interval as QTL identified with joint linkage analysis (data not shown).

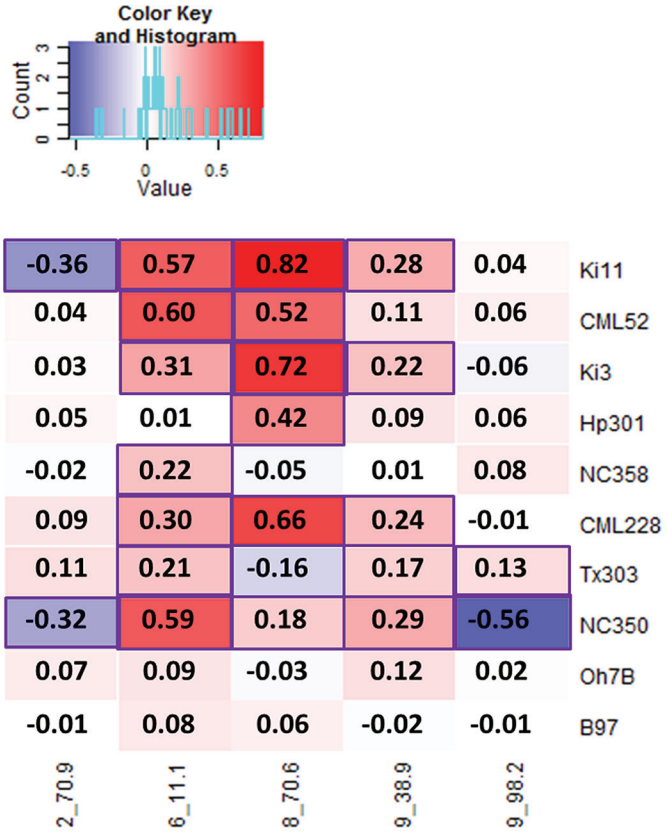

Figure 2. Heat map for kernel color quantitative trait loci (QTL) effects by chromosome and position in centimorgans (Chr_cM) and QTL donor. The diverse parents are ordered from highest to lowest kernel color best linear unbiased predictor. The diverse parents with darker orange kernel color tend to have stronger positive effect QTL relative to those with kernels that are yellow or light orange but also have QTL with a moderate-to-weak negative effect. All statistically significant effects at a false discovery rate of 5% are indicated by a purple rectangle border.

Table 2. Summary of joint linkage analysis across the 10 nested association mapping families.

Chr.†	Peak position, cM	Support interval, cM	Marker at the peak	Peak LOD‡	PVE (%)§	Candidate genes¶
2	70.9	69.4–71.3	PZA01820.1	21.47	6.6	*zep1*#
6	11.1	10.7–11.3	PZA00355.2	88.22	20.7	*y1*
8	70.6	70.6–71.6	PZA00090.1	132.54	38.3	*lcyε*#
9	38.9	38.9–40.0	zb7.2	23.99	5.3	
9	98.2	94.8–101.2	PHM4303.16	24.98	8.7	*ccd1*

†Chr., chromosome.

‡The logarithm of odds (LOD) value at the position of peak likelihood of the QTL.

§Phenotypic variance explained (PVE) by each quantitative trait loci (QTL). Because of the possible linkage between identified QTL, the total genotypic variance explained by all identified QTL cannot be considered identical to the sum of genotypic variance explained by individual QTL (Li et al., 2011).

¶AGPv2 coordinates for candidate genes: *zep1* (chromosome 2: 44,440,299–44,449,237 bp), *y1* (chromosome 6: 82,017,148–82,021,007 bp), *lcyε* (chromosome 8:138,882,594–138,889,812 bp), and *ccd1* (chromosome 9: 152,086,899–152,092,882 bp).

#Candidate gene located within the QTL support interval.

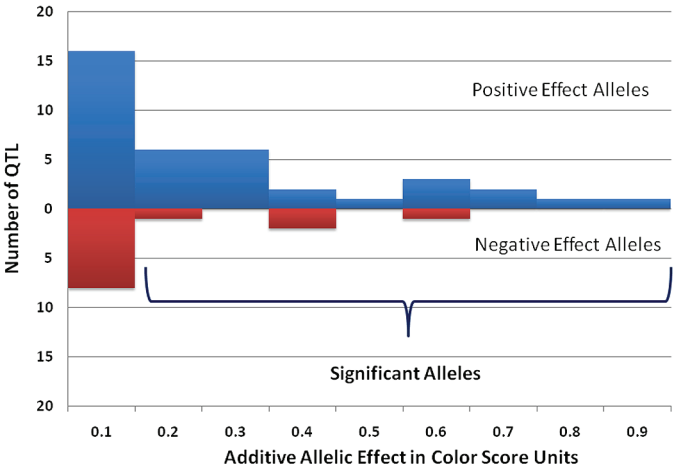

Figure 3. Quantitative trait loci (QTL) effect size distribution in color score units. Nearly 95% of the effects are less than 0.75 color score units. Only 46% of the QTL have a significant effect at a false discovery rate of 5%, and the significant effects range from 0.13 to 0.82 color score units.

We tested for environmental interactions in a joint analysis, and only two of the five QTL had a significant interaction, by showing significantly different effect sizes between environments. The QTL on chromosome 6 had a highly significant interaction with the environment ($P = 5.60 \times 10^{-21}$) followed by the QTL at 38.9 cM on chromosome 9 ($P = 6.60 \times 10^{-4}$). When fitted in a random effects model, these two significant interaction terms accounted for less than 5% of the total phenotypic variance. For both QTL, genetic variance was nearly threefold greater than interaction variance, illustrating that genetic variance had a much larger role than Q×E interaction variance for kernel color in the 10 NAM families when grown for 2 yr at a single location (Supplemental Table S2). We also tested for epistatic interactions among all marker pairs in a combined analysis of the 10 NAM families and within each family separately. Neither the joint analysis nor single family analysis detected any significant pairwise epistatic interactions.

Carotenoid Biosynthetic and Degradation Genes within Quantitative Trait Loci Regions

We assessed whether known genes involved in carotenoid biosynthesis or cleavage colocalized with the genomic position of identified QTL. Four of the five QTL identified by joint-linkage analysis were associated with a carotenoid biosynthetic or degradation gene (Fig. 4; Table 2). The lycopene epsilon cyclase (*lcyE*) gene on chromosome 8 was within the support interval of the QTL with the largest PVE, and the zeaxanthin epoxidase 1 (*zep1*) gene resided within the support interval of the QTL on chromosome 2. The support interval for the QTL on chromosome 6 did not contain a logical candidate gene, but a gene encoding phytoene synthase 1 (*y1* or *psy1*) was located approximately 2.1 Mbp from the QTL peak. In addition, the support interval for the more distal QTL on chromosome 9 (98.2 cM) did not contain a likely candidate gene, but the carotenoid cleavage dioxygenase 1 (*ccd1* or *wc1*) gene was located approximately 1.3 Mbp from the QTL peak.

We identified two rare QTL with single family linkage analysis that were associated with a carotenoid biosynthetic gene (Table 3). The support interval of the rare QTL on chromosome 7 in the B73 × B97 family contained the ζ-carotene desaturase 1 (*zds1*) gene. For the B73 × Tx303 family, the support interval for the QTL on chromosome 10 did not contain a candidate gene, but the β-carotene hydroxylase 1 (*crtRB1* or *HYD3*) gene was located approximately 236 Kbp from the QTL peak. In concordance with joint linkage analysis results, *y1*, *lcyE*, *zep1*, and *ccd1* were associated with common QTL that were also independently identified by single family linkage analysis.

DISCUSSION

We assessed the extent to which visual scores for gradation in orange kernel color were heritable across and within 10 families from the maize NAM population. Although the 10 NAM families were evaluated for only 2 yr at a single location, the $\hat{h}_l^2$ of kernel color across the 10 NAM families was moderately high at 0.78. Heritability on an individual plot basis across all NAM families ($\hat{h}_p^2$) across the 10 NAM families was just 9% lower than line-mean basis heritability, indicating that field evaluation of the NAM lines for a second year did not substantially increase mean heritability at this location. On average, $\hat{h}_{lw_p}^2$ was moderately high at 0.64. These estimates of heritability suggest that variation for kernel color within a family was influenced mainly by QTL, and kernel color should respond favorably to selection based on line means when using the experimental design that was used in this study (Holland et al., 2003).

We identified QTL associated with visually scored orange kernel color through linkage analysis combined across the 10 NAM families and within each family. Five QTL with mostly small effects accounted for the vast majority of genetic variance for kernel color among the 10 NAM families. At least two of these QTL had both positive and negative effects relative to B73, which may have been the result of an allelic series (i.e., multiple functional polymorphisms per locus), rare alleles distributed across a cluster of tightly linked QTL, or higher order epistasis (Buckler et al., 2009; Chardon et al., 2005; Harjes et al., 2008; Mackay, 2004). The five QTL did not show significant pairwise epistatic interactions or environmental interactions with large effects; therefore, a simple additive genetic model adequately accounted for variation in orange kernel color. In addition to the five QTL identified by joint linkage analysis, another six putative rare QTL with small effects were associated with phenotypic variation within families. These rare QTL may have been at a higher frequency if all 25 NAM families had been analyzed.

Table 3. Summary of linkage analysis within each of the 10 nested association mapping families.

Family	Chr.†	Peak position, cM	Support interval, cM	Marker at the peak	Peak LOD‡	Additive effects§	PVE (%)¶	Candidate genes#
B73 × B97	2	8.5	5.7–11.5	PZB01233.1	6.38	0.12	11.5	
	6	11.8	10.7–13.1	PZA02606.1	3.55	0.09	6.5	*y1*††
	7	39.9	39.9–43.9	PZA02872.1	11.58	−0.18	26.9	*zds1*††
B73 × CML228	6	13.1	11.7–13.1	PHM2551.31	6.92	0.33	10.1	*y1*
	8	70.6	70.6–71.6	PZA00090.1	21.14	0.66	39.6	*lcyε*
	9	40	38.9–40	PZB00547.3	3.57	0.24	5.2	
B73 × CML52	6	10.7	10.7–11.8	PZA01425.2	15.67	0.62	34.5	*y1*††
	8	70.6	70.6–71.6	PZA00090.1	11.56	0.50	22.8	*lcyε*††
B73 × Hp301	8	70.6	69.7–71.6	PZA00090.1	15.53	0.42	35.7	*lcyε*††
B73 × Ki11	2	70.9	70.9–73.6	PZA01820.1	6.26	−0.39	7.6	*zep1*
	6	10.7	8.8–12.4	PZA01425.2	10.47	0.52	13.5	*y1*††
	8	69	68–69.8	PHM14152.18	22.98	0.84	34.8	*lcyε*
	9	34.5	32.6–34.5	PZA03058.22.21	4.37	0.33	5.4	
B73 × Ki3	5	60.6	60.6–63.6	PZA02207.1	3.94	−0.32	7.9	
	6	18.6	10.7–18.6	PHM8909.12	4.44	0.37	10.1	*y1*††
	8	69.8	69.7–70.6	PHM448.23	15.04	0.69	35.5	*lcyε*
B73 × NC350	2	71.3	69.4–71.3	PZA02774.1	4.91	−0.30	6.4	*zep1*††
	3	115.8	111.2–115.8	PZA00538.18.15	3.44	0.25	4.3	
	6	11.1	11.1–11.3	PZA00355.2	15.17	0.57	23.2	*y1*
	9	47	46.6–49.1	PZA01062.1	5.10	0.31	7.0	
	9	98.2	94.8–98.2	PHM4303.16	13.67	−0.57	23.1	*ccd1*
B73 × NC358	6	11.3	10.7–12.4	PZA00543.12	10.87	0.23	27.7	*y1*††
B73 × Oh7B	2	84.2	84.2–85.5	PZA03644.1	4.00	0.14	9.5	
	6	11.8	10.7–18.6	PZA02606.1	3.61	0.12	7.6	*y1*††
	7	77	76.5–81.2	PZA00405.7.6	6.02	−0.16	13.3	
	9	34.5	32.6–34.5	PZA03058.22.21	5.87	0.15	12.3	
B73 × Tx303	4	112.5	111.3–116.1	PZA00636.7	3.40	0.17	5.5	
	6	7.1	6.9–8.8	PZA00440.15.1	7.23	0.25	11.8	*y1*
	8	17.6	17.1–18.3	PZA00058.1	6.51	−0.24	11.1	
	9	47.2	46.6–47.2	PZA03596.1	5.06	0.21	8.5	
	10	61.6	61.6–63	PZA01456.2	3.81	−0.17	6.0	*crtRB1*

†Chr., chromosome.

‡The logarithm of odds (LOD) value at the position of peak likelihood of the QTL.

§Additive effect when substituting allele from B73 parent with allele from non-B73 parent.

¶Phenotypic variance explained (PVE) by each quantitative trait loci (QTL).

#AGPv2 coordinates for rare candidate genes: *crtRB1* (chromosome 10: 136,057,100–136,060,219 bp) and *zds1* (chromosome 7: 17,470,585–17,479,020 bp).

††Candidate gene located within the QTL support interval.

The apparent oligogenic basis of the orange kernel color trait is consistent with that of yellow grain color in sorghum [*Sorghum bicolor* (L.) Moench] (Fernandez et al., 2008) and durum wheat (*Triticum durum* Desf.) (Pozniak et al., 2007) but clearly contrasts the complex architecture of maize flowering time, leaf architecture, inflorescence architecture, kernel composition, and foliar fungal resistance traits that are underpinned by 21 to 39 QTL in the maize NAM population (Brown et al., 2011; Buckler et al., 2009; Cook et al., 2012; Kump et al., 2011; Poland et al., 2011; Tian et al., 2011). These complex traits are similar to orange kernel color in that they are predominantly controlled by small additive effects with minimal epistatic or environmental interactions and show both positive and negative effect QTL relative to B73. Although orange kernel color seems to be an oligogenic trait, it is possible that a few additional minor QTL would have been identified if more than 10 NAM families were analyzed, the trait was scored on a continuous color scale, and additional environments were used for field evaluations. In addition, Q×E interaction variance could be a relatively larger component of the genetic architecture in more climatically different environments.

The QTL on chromosome 6 that accounted for 21% of the phenotypic variance in the joint linkage analysis was in

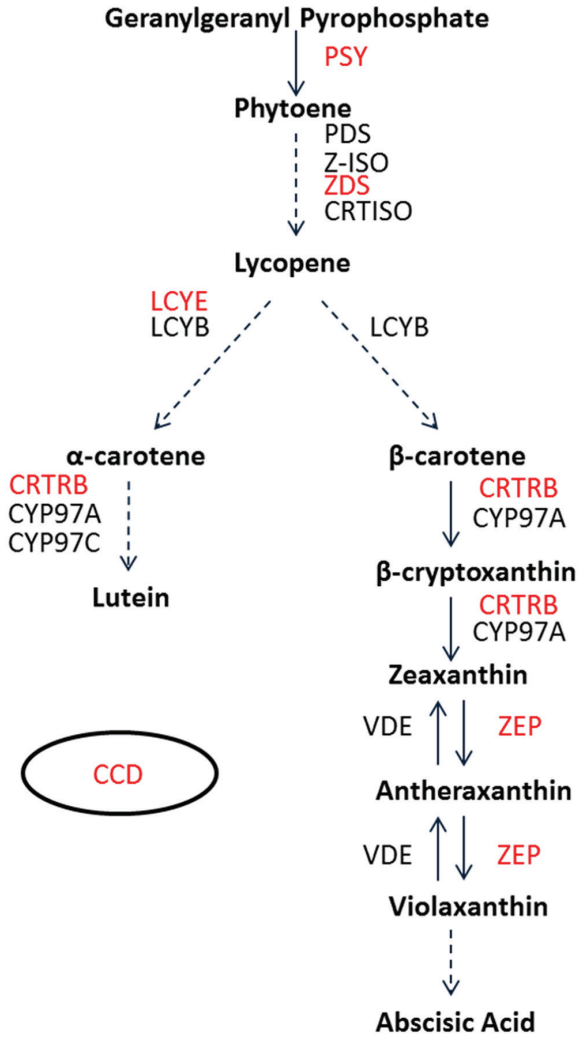

Figure 4. The carotenoid biosynthetic pathway in the maize kernel. Solid arrows are single reactions and dashed arrows represent two or more reactions. The enzymes in red correspond to biosynthetic genes in the vicinity of quantitative trait loci (QTL) discovered in this study, and the enzymes in black represent the minimum activities required for the pathway. The circled enzyme is not part of the biosynthetic pathway but degrades carotenoids. Note that for some steps there are multiple paralogs for a reaction. PSY, phytoene synthase; PDS, phytoene desaturase; Z-ISO, ζ-carotene isomerase; ZDS, ζ-carotene desaturase; CRTISO, carotenoid isomerase; LCYE, lycopene ε-cyclase; LCYB, lycopene β-cyclase; CYP97A, β-carotene hydroxylase (P450); CYP97C, ε-carotene hydroxylase (P450); CRTRB, β-carotene hydroxylase; VDE, violaxanthin de-epoxidase; ZEP, zeaxanthin epoxidase; CCD, carotenoid cleavage dioxygenase.

the vicinity of the *y1* gene. The phytoene synthase (PSY) enzyme encoded by *y1* is involved in the first dedicated step of the carotenoid pathway in the maize endosperm. Presence of the null *y1* allele versus the functional *Y1* allele is responsible for the qualitative color difference between white and yellow kernels, respectively (Buckner et al., 1990, 1996). Quantitative trait loci associated with quantitative variation for kernel carotenoids were identified near the *y1* gene in a maize mapping population (W64a × A632) that also segregated for gradation in yellow kernel color (Wong et al., 2004). Our study suggests that *Y1* alleles are a contributor to orange kernel color. Phytoene synthase 1 is involved in the first committed step of the carotenoid pathway in the maize endosperm; therefore, allelic variation associated with increased enzyme activity could contribute to darker orange color by increasing flux into the pathway.

We detected a rare QTL on chromosome 7 in B73 × B97 that was coincident with the *zds1* gene. Notably, Wong et al. (2004) also detected a major QTL for accumulation of carotenoids in maize kernels that colocalized with *zds1* in the W64a × A632 population. The QTL associated with *zds1* in B73 × B97 may not be rare but segregated at a low frequency in the 10 NAM families. The desaturation of 9,9′-di-cis-ζ-carotene is catalyzed by ZDS, which in combination with carotenoid isomerase (CRTISO) results in the formation of *all*-trans lycopene—the first colored carotenoid in the pathway (Chen et al., 2010; Li et al., 2007; Matthews et al., 2003). Given that ZDS directs flux from the colorless to the colored part of the pathway, *zds1* is a plausible candidate gene for gradation in orange kernel color.

The QTL on chromosome 8 explained the largest proportion of phenotypic variation (~38%) across the 10 NAM families and coincided with the *lcyE* gene. The lycopene ε-cyclase (LCYE) enzyme plays a key role in the carotenoid pathway (Fig. 4), influencing flux of compounds into either the α- or β-carotene branch of the pathway (Cunningham et al., 1996). Weak alleles of *lcyE* have been associated with favorably increasing the ratio of the sum of the β branch carotenoids to the sum of the α branch carotenoids in the maize kernel (Harjes et al., 2008). The β branch carotenoids have a slightly more orange color than α branch carotenoids (Britton et al., 2004) and this contributes to the darker orange kernel color associated with weak alleles of *lcyE* (Harjes et al., 2008). Marker-assisted selection on these weak *lcyE* alleles should also increase the pool of provitamin A precursors by enhancing flux into the β-carotene branch of the pathway. Preliminary data indicate that visual selection for dark orange kernel color within maize breeding programs results in slightly higher content of provitamin A compounds, but further research is needed to determine if the increase is directly from the fixation of favorable *lcyE* alleles (Kandianis, 2009; Stevens, 2004).

A rare QTL discovered in B73 × Tx303 was in the vicinity of the *crtRB1* gene on chromosome 10. The β-carotene hydroxylase (CRTRB) enzyme is responsible for the hydroxylation of β-carotene to β-cryptoxanthin and zeaxanthin (Sun et al., 1996; Tian and DellaPenna, 2001). This has implications for provitamin A biofortification efforts because β-cryptoxanthin and zeaxanthin have 50 and 0% of the provitamin A activity of β-carotene, respectively (Institute of Medicine, 2000). Polymorphisms

within *crtRB1* have been significantly associated with β-carotene concentration and conversion in maize kernels (Yan et al., 2010). Yan et al. (2010) showed that *crtRB1* alleles associated with higher β-carotene concomitantly decreased total carotenoid content in the kernel, indicating that selection for *crtRB1* alleles that increase β-carotene will result in a decrease of orange color. Indeed, this was observed when conducting MAS for favorable *crtRB1* alleles (C. Kandianis and T. Rocheford, personal communication, 2009). Therefore, concurrent selection for orange kernel color is needed to increase flux into and throughout the carotenoid pathway in combination with selection for *crtRB1* alleles that increase β-carotene.

We identified two QTL in joint linkage analysis that were each in the vicinity of a candidate gene associated with a reduction in the amount of carotenoids in the kernel. The QTL on chromosome 2 was coincident with the *zep1* gene, and it had significant negative effects for decreased orange color across the 10 NAM families (Fig. 2). The formation of violaxanthin from zeaxanthin via the intermediate antheraxanthin results from the activity of zeaxanthin epoxidase (ZEP). The higher expression of ZEP is negatively correlated with carotenoid content in the maize kernel because the eventual formation of abscisic acid, which requires ZEP (Fig. 4), depletes the endosperm carotenoid pool (Vallabhaneni and Wurtzel, 2009). The QTL at 98.2 cM on chromosome 9 was in close proximity to a gene that encoded a carotenoid cleavage dioxygenase (CCD), an enzyme that cleaves carotenoids in the maize endosperm (Vogel et al., 2008). This QTL had both significant positive and negative effects relative to B73 across the 10 NAM families (Fig. 2). The dominant White Cap 1 (*Wc1*) maize mutant has a tandem array of several CCD copies and diminishes endosperm carotenoid content on the crown of the kernel (Tan et al., 2004). Taken together, weak alleles of *zep1* and *ccd1* may lead to higher total carotenoids and darker orange color.

SUMMARY AND PERSPECTIVES

The moderately high heritability of visual scores for relative intensity of orange kernel color indicates that this trait should respond favorably to phenotypic selection. The identification of strong positive effect QTL in the vicinity of carotenoid biosynthetic pathway genes *y1*, *zds1*, and *lcyE* implies that phenotypic selection for dark orange color will likely result in higher amounts of total carotenoids in the maize kernel. However, the discovery of only weak positive effect QTL in close proximity to *zep1* and *ccd1* underscores the need to further explore and characterize genetic diversity at these two loci and search for more favorable alleles. Phenotypic selection for orange color should be effective, simple, and low cost for converting white or yellow grain maize germplasm to orange. To further enhance β-carotene levels, this phenotypic selection could be combined with MAS for favorable *crtRB1* alleles. Genotyping single kernels and selecting for favorable alleles at the six loci would further expedite breeding efforts by assuring that the most desirable genotypes are selected before planting in winter or summer nurseries. Such an approach could be combined with a strategy that uses a set of genomewide markers to rapidly select against the undesirable genetic background of less adapted or lower yielding orange donor lines. In summary, this study provides useful information that enables flexibility for maize provitamin A biofortification breeding approaches.

Supplemental Information Available

Supplemental material is available at http://www.crops.org/publications/cs.

Supplemental Table S1. Variance component estimates of statistically significant terms in random effects model fitted to estimate best linear unbiased predictors (BLUPs).

Supplemental Table S2. Summary of variance component estimates from genotype × environment (G×E) ASReml analysis (Gilmour et al., 2009).

Acknowledgments

This research was supported by National Science Foundation (NSF) DBI-0321467 (E.S.B.), DBI-0820619 (E.S.B.), DBI-0922493 (E.S.B. and T.R.), Pioneer Hi-Bred Graduate Research Assistantship (K.C.), HarvestPlus CGIAR Grand Challenge Program (T.R.), and USDA-ARS (M.A.G. and E.S.B.). Mention of trade names or commercial products in this publication is solely for the purpose of providing specific information and does not imply recommendation or endorsement by the USDA. The USDA is an equal opportunity provider and employer. We especially thank Dean DellaPenna for valuable insights on the carotenoid biosynthetic pathway in maize. Also, we wish to thank Cathy Kandianis for critical evaluation of the manuscript.

References

Benjamini, Y., and Y. Hochberg. 1995. Controlling the false discovery rate: A practical and powerful approach to multiple testing. J. Roy. Stat. Soc. B. Met. 57:289–300.

Bouis, H.E., and R.M. Welch. 2010. Biofortification – A sustainable agricultural strategy for reducing micronutrient malnutrition in the global south. Crop Sci. 50:S-20–S-32. doi:10.2135/cropsci2009.09.0531

Britton, G., S. Liaaen-Jensen, and H. Pfander. 2004. Carotenoids handbook. Birkhäuser Verlag, Basel, Switzerland.

Brown, P.J., N. Upadyayula, G.S. Mahone, F. Tian, P.J. Bradbury, S. Myles, J.B. Holland, S. Flint-Garcia, M.D. McMullen, E.S. Buckler, and T.R. Rocheford. 2011. Distinct genetic architectures for male and female inflorescence traits of maize. PLoS Genet. 7:e1002383. doi:10.1371/journal.pgen.1002383

Buckler, E.S., J.B. Holland, P.J. Bradbury, C.B. Acharya, P.J. Brown, C. Browne, E. Ersoz, S. Flint-Garcia, A. Garcia, J.C. Glaubitz, M.M. Goodman, C. Harjes, K. Guill, D.E. Kroon, S. Larsson, N.K. Lepak, H. Li, S.E. Mitchell, G. Pressoir, J.A. Peiffer, M.O. Rosas, T.R. Rocheford, M.C. Romay, S. Romero, S. Salvo,

H.S. Villeda, H. Sofia da Silva, Q. Sun, F. Tian, N. Upadyayula, D. Ware, H. Yates, J. Yu, Z. Zhang, S. Kresovich, and M.D. McMullen. 2009. The genetic architecture of maize flowering time. Science 325:714–718. doi:10.1126/science.1174276

Buckner, B., T.L. Kelson, and D.S. Robertson. 1990. Cloning of the *y1* locus of maize, a gene involved in the biosynthesis of carotenoids. Plant Cell 2:867–876.

Buckner, B., P.S. Miguel, D. Janick-Buckner, and J.L. Bennetzen. 1996. The *y1* gene of maize codes for phytoene synthase. Genetics 143:479–488.

Chardon, F., D. Hourcade, V. Combes, and A. Charcosset. 2005. Mapping of a spontaneous mutation for early flowering time in maize highlights contrasting allelic series at two linked QTL on chromosome 8. Theor. Appl. Genet. 112:1–11. doi:10.1007/s00122-005-0050-z

Chen, Y., F. Li, and E.T. Wurtzel. 2010. Isolation and characterization of the Z-ISO gene encoding a missing component of carotenoid biosynthesis in plants. Plant Physiol. 153:66–79. doi:10.1104/pp.110.153916

Churchill, G.A., and R.W. Doerge. 1994. Empirical threshold values for quantitative trait mapping. Genetics 138:963–971.

Cook, J.P., M.D. McMullen, J.B. Holland, F. Tian, P. Bradbury, J. Ross-Ibarra, E.S. Buckler, and S.A. Flint-Garcia. 2012. Genetic architecture of maize kernel composition in the nested association mapping and inbred association panels. Plant Physiol. 158:824–834. doi:10.1104/pp.111.185033

Cullis, B.R., A. Smith, and N. Coombes. 2006. On the design of early generation variety trials with correlated data. J. Agric. Biol. Environ. Stat. 11:381–393. doi:10.1198/108571106X154443

Cunningham, F.X., Jr., B. Pogson, Z. Sun, K.A. McDonald, D. DellaPenna, and E. Gantt. 1996. Functional analysis of the β- and ε-lycopene cyclase enzymes of *Arabidopsis* reveals a mechanism for control of cyclic carotenoid formation. Plant Cell 8:1613–1626.

De Groote, H., and S.C. Kimenju. 2008. Comparing consumer preferences for color and nutritional quality in maize: Application of a semi-double-bound logistic model on urban consumers in Kenya. Food Policy 33:362–370. doi:10.1016/j.foodpol.2008.02.005

Fernandez, M.G.S., M.T. Hamblin, L. Li, W.L. Rooney, M.R. Tuinstra, and S. Kresovich. 2008. Quantitative trait loci analysis of endosperm color and carotenoid content in sorghum grain. Crop Sci. 48:1732–1743. doi:10.2135/cropsci2007.12.0684

Flint-Garcia, S.A., A.-C. Thuillet, J. Yu, G. Pressoir, S.M. Romero, S.E. Mitchell, J. Doebley, S. Kresovich, M.M. Goodman, and E.S. Buckler. 2005. Maize association population: A high-resolution platform for quantitative trait locus dissection. Plant J. 44:1054–1064. doi:10.1111/j.1365-313X.2005.02591.x

Gilmour, A.R., B.J. Gogel, B.R. Cullis, and R. Thompson. 2009. ASReml user guide release 3.0. VSN International Ltd., Hemel Hempstead, UK.

Graham, R.D., R.M. Welch, and H.E. Bouis. 2001. Addressing micronutrient malnutrition through enhancing the nutritional quality of staple foods: Principles, perspectives and knowledge gaps. Adv. Agron. 70:77–142.

Harjes, C.E., T.R. Rocheford, L. Bai, T.P. Brutnell, C.B. Kandianis, S.G. Sowinski, A.E. Stapleton, R. Vallabhaneni, M. Williams, E.T. Wurtzel, J. Yan, and E.S. Buckler. 2008. Natural genetic variation in lycopene epsilon cyclase tapped for maize biofortification. Science 319:330–333. doi:10.1126/science.1150255

Holland, J.B., W.E. Nyguist, and C.T. Cervantes-Martinez. 2003. Estimating and interpreting heritability for plant breeding: An update. Plant Breed. Rev. 22:9–112.

Hung, H.Y., C. Browne, K. Guill, N. Coles, M. Eller, A. Garcia, N. Lepak, S. Melia-Hancock, M. Oropeza-Rosas, S. Salvo, N. Upadyayula, E.S. Buckler, S. Flint-Garcia, M.D. McMullen, T.R. Rocheford, and J.B. Holland. 2012. The relationship between parental genetic or phenotypic divergence and progeny variation in the maize nested association mapping population. Heredity 108:490–499. doi:10.1038/hdy.2011.103

Institute of Medicine. 2000. Beta-carotene and other carotenoids. Dietary reference intakes for vitamin C, vitamin E, selenium, and carotenoids. National Academy Press, Washington, DC. p. 325–400.

Institute of Medicine. 2012. Dietary reference intakes (DRIs): Estimated average requirements. Food and Nutrition Board, Institute of Medicine, Washington, DC. http://www.iom.edu/Activities/Nutrition/SummaryDRIs/~/media/Files/Activity%20Files/Nutrition/DRIs/5_Summary%20Table%20Tables%201-4.pdf (accessed 12 May 2012).

Kandianis, C. 2009. Genetic dissection of carotenoid concentration and compositional traits in maize grain. Ph.D. diss. University of Illinois at Urbana-Champaign, Urbana, IL.

Kump, K.L., P.J. Bradbury, R.J. Wisser, E.S. Buckler, A.R. Belcher, M.A. Oropeza-Rosas, J.C. Zwonitzer, S. Kresovich, M.D. McMullen, D. Ware, P.J. Balint-Kurti, and J.B. Holland. 2011. Genome-wide association study of quantitative resistance to southern leaf blight in the maize nested association mapping population. Nat. Genet. 43:163–168. doi:10.1038/ng.747

Lee, M., N. Sharopova, W.D. Beavis, D. Grant, M. Katt, D. Blair, and A. Hallauer. 2002. Expanding the genetic map of maize with the intermated B73 × Mo17 (IBM) population. Plant Mol. Biol. 48:453–461. doi:10.1023/A:1014893521186

Li, F., C. Murillo, and E.T. Wurtzel. 2007. Maize Y9 encodes a product essential for 15-cis-ζ-carotene isomerization. Plant Physiol. 144:1181–1189. doi:10.1104/pp.107.098996

Li, H., P. Bradbury, E. Ersoz, E.S. Buckler, and J. Wang. 2011. Joint QTL linkage mapping for multiple-cross mating design sharing one common parent. PLoS ONE 6:e17573. doi:10.1371/journal.pone.0017573

Littell, R.C., G.A. Milliken, W.W. Stroup, and R. Wolfinger. 1996. SAS system for mixed models. SAS Publishing: Cary, NC.

Mackay, T.F.C. 2004. The genetic architecture of quantitative traits: Lessons from *Drosophila*. Curr. Opin. Genet. Dev. 14:253–257. doi:10.1016/j.gde.2004.04.003

Matthews, P.D., R. Luo, and E.T. Wurtzel. 2003. Maize phytoene desaturase and ζ-carotene desaturase catalyse a poly-Z desaturation pathway: Implications for genetic engineering of carotenoid content among cereal crops. J. Exp. Bot. 54:2215–2230. doi:10.1093/jxb/erg235

McMullen, M.D., S. Kresovich, H.S. Villeda, P. Bradbury, H. Li, Q. Sun, S. Flint-Garcia, J. Thornsberry, C. Acharya, C. Bottoms, P. Brown, C. Browne, M. Eller, K. Guill, C. Harjes, D. Kroon, N. Lepak, S.E. Mitchell, B. Peterson, G. Pressoir, S. Romero, M. Oropeza Rosas, S. Salvo, H. Yates, M. Hanson, E. Jones, S. Smith, J.C. Glaubitz, M. Goodman, D. Ware, J.B. Holland, and E.S. Buckler. 2009. Genetic properties of the maize nested association mapping population. Science 325:737–740. doi:10.1126/science.1174320

Meenakshi, J.V., A. Banerji, V. Manyong, K. Tomlins, N. Mittal, and P. Hamukwala. 2012. Using a discrete choice experiment to elicit the demand for a nutritious food: Willingness-to-pay for orange maize in rural Zambia. J. Health Econ. 31:62–71. doi:10.1016/j.jhealeco.2012.01.002

Mora, J.O. 2003. Proposed vitamin A fortification levels. J. Nutr. 133:2990S–2993S.

Muzhingi, T., A.S. Langyintuo, L.C. Malaba, and M. Banziger. 2008. Consumer acceptability of yellow maize products in Zimbabwe. Food Policy 33:352–361. doi:10.1016/j.foodpol.2007.09.003

Pillay, K., J. Derera, M. Siwela, and F.J. Veldman. 2011. Consumer acceptance of yellow, provitamin A-biofortified maize in KwaZulu-Natal. S. Afr. J. Clin. Nutr. 24:186–191.

Poland, J.A., P.J. Bradbury, E.S. Buckler, and R.J. Nelson. 2011. Genome-wide nested association mapping of quantitative resistance to northern leaf blight in maize. Proc. Natl. Acad. Sci. USA 108:6893–6898. doi:10.1073/pnas.1010894108

Pozniak, C.J., R.E. Knox, F.R. Clarke, and J.M. Clarke. 2007. Identification of QTL and association of a phytoene synthase gene with endosperm colour in durum wheat. Theor. Appl. Genet. 114:525–537. doi:10.1007/s00122-006-0453-5

Quackenbush, F.W., J.G. Firch, W.J. Rabourn, M. McQuistan, W.N. Petzold, and T.E. Kargl. 1961. Composition of corn, analysis of carotenoids in corn grain. J. Agric. Food Chem. 9:132–135. doi:10.1021/jf60114a012

Ross, D.A. 2002. Recommendations for vitamin A supplementation. J. Nutr. 132:2902S–2906S.

SAS Institute. 2011. The SAS system for Windows. Release 9.2. SAS Inst., Cary, NC

Sommer, A. 1995. Vitamin A deficiency and its consequences. A field guide to detection and control, 3rd ed. World Health Organization., Geneva, Switzerland.

Sommer, A., G. Hussaini, I. Tarwotjo, D. Susanto, and T. Soegiharto. 1981. Incidence, prevalence, and scale of blinding malnutrition. Lancet 317:1407–1408. doi:10.1016/S0140-6736(81)92581-2

Stevens, R. 2004. Genetic and QTL analysis of carotenoid variation in two mapping populations of maize. M.S., thesis. University of Illinois at Urbana-Champaign, Urbana, IL.

Stevens, R., and A. Winter-Nelson. 2008. Consumer acceptance of provitamin A-biofortified maize in Maputo, Mozambique. Food Policy 33:341–351. doi:10.1016/j.foodpol.2007.12.003

Sun, Z., E. Gantt, and F.X.J. Cunningham. 1996. Cloning and functional analysis of the β-carotene hydroxylase of *Arabidopsis thaliana*. J. Biol. Chem. 271:24349–24352. doi:10.1074/jbc.271.40.24349

Tan, B.-C., L. Liu, S. Wu, J. Lai, A. Simone, and D. McCarty. 2004. The dominant white endosperm factor white cap encodes the ZmCCD1 carotenoid dioxygenase in a large multiple copy gene array. Talk given at the 46th Annual Maize Genetics Conference, Mexico City, Mexico. 11–14 Mar. 2004. Talk 14.

Tian, F., P.J. Bradbury, P.J. Brown, H. Hung, Q. Sun, S. Flint-Garcia, T.R. Rocheford, M.D. McMullen, J.B. Holland, and E.S. Buckler. 2011. Genome-wide association study of leaf architecture in the maize nested association mapping population. Nat. Genet. 43:159–162. doi:10.1038/ng.746

Tian, L., and D. DellaPenna. 2001. Characterization of a second carotenoid β-hydroxylase gene from *Arabidopsis* and its relationship to the LUT1 locus. Plant Mol. Biol. 47:379–388. doi:10.1023/A:1011623907959

Underwood, B., and P. Arthur. 1996. The contribution of vitamin A to public health. FASEB J. 10:1040–1048.

Vallabhaneni, R., and E.T. Wurtzel. 2009. Timing and biosynthetic potential for carotenoid accumulation in genetically diverse germplasm of maize. Plant Physiol. 150:562–572. doi:10.1104/pp.109.137042

Vogel, J.T., B.-C. Tan, D.R. McCarty, and H.J. Klee. 2008. The carotenoid cleavage dioxygenase 1 enzyme has broad substrate specificity, cleaving multiple carotenoids at two different bond positions. J. Biol. Chem. 283:11364–11373. doi:10.1074/jbc.M710106200

Weber, E. 1987. Carotenoids and tocols of corn grain determined by HPLC. J. Am. Oil Chem. Soc. 64:1129–1134. doi:10.1007/BF02612988

Welch, R.M., and R.D. Graham. 2004. Breeding for micronutrients in staple food crops from a human nutrition perspective. J. Exp. Bot. 55:353–364. doi:10.1093/jxb/erh064

West, C.E. 2000. Meeting requirements for vitamin A. Nutr. Rev. 58:341–345. doi:10.1111/j.1753-4887.2000.tb01831.x

West, C.E., A. Eilander, and M. van Lieshout. 2002. Consequences of revised estimates of carotenoid bioefficacy for dietary control of vitamin A deficiency in developing countries. J. Nutr. 132:2920S–2926S.

West, K.P. 2002. Extent of vitamin A deficiency among preschool children and women of reproductive age. J. Nutr. 132:2857S–2866S.

West, K.P., and I. Darnton-Hill. 2008. Vitamin A deficiency. In: R. D. Semba and M. Bloem, editors, Nutrition and health in developing countries, 2nd ed. The Humana Press, Inc., Totowa, NJ. p. 377–433.

Wong, J.C., R.J. Lambert, E.T. Wurtzel, and T.R. Rocheford. 2004. QTL and candidate genes phytoene synthase and zeta-carotene desaturase associated with the accumulation of carotenoids in maize. Theor. Appl. Genet. 108:349–359. doi:10.1007/s00122-003-1436-4

Yan, J., C.B. Kandianis, C.E. Harjes, L. Bai, E.-H. Kim, X. Yang, D.J. Skinner, Z. Fu, S. Mitchell, Q. Li, M.G.S. Fernandez, M. Zaharieva, R. Babu, Y. Fu, N. Palacios, J. Li, D. DellaPenna, T. Brutnell, E.S. Buckler, M.L. Warburton, and T. Rocheford. 2010. Rare genetic variation at *Zea mays* crtRB1 increases β-carotene in maize grain. Nat. Genet. 42:322–327. doi:10.1038/ng.551

Yu, J., J.B. Holland, M.D. McMullen, and E.S. Buckler. 2008. Genetic design and statistical power of nested association mapping in maize. Genetics 178:539–551. doi:10.1534/genetics.107.074245